Identification of a Surface Alkylperoxy Radical in the Photocatalytic Oxidation of Acetone/O_2 over TiO_2

Anna L. Attwood,[†] John L. Edwards,[‡] Christopher C. Rowlands,[†] and Damien M. Murphy*[,†]

Department of Chemistry, Cardiff University, P.O. Box 912, Cardiff, CF10 3TB, United Kingdom, and Huntsman Tioxide, Haverton Hill Road, Billingham TS23 IPS, United Kingdom

Received: November 15, 2002

The interaction of a coadsorbed mixture of acetone and oxygen with a clean oxidized polycrystalline sample of TiO_2 (P25) was investigated using electron paramagnetic resonance (EPR) spectroscopy. UV illumination of the sample at low temperature (100 K) generated an unstable radical intermediate at the dehydrated (and hydrated) TiO_2 surface. The radical decayed irreversibly at temperatures greater than 150 K but was regenerated by subsequent irradiation at low temperatures. Using a series of isotopically labeled gases (CH_3COCH_3, CD_3-$COCD_3$, $^{16}O_2$, and $^{17}O_2$) to aid in the interpretation of the EPR spectrum, the radical was identified as an alkylperoxy species $RCH_2OO^{\bullet}$ with the spin Hamiltonian parameters of $g_1 = 2.0345$, $g_2 = 2.0070$, $g_3 = 2.0010$, $^{H}A_1 = 0.34$ mT, $^{H}A_2 = 0.10$ mT, $^{H}A_3 = 0.29$ mT, $^{17O}A_{||}(i) = 9.45$ mT (for $RO^{17}O^{\bullet}$), and $^{17O}A_{||}(ii) = 5.52$ mT (for $R^{17}OO^{\bullet}$). By consideration of the different mechanistic pathways involved in the oxidation of acetone, it was concluded that the observed radical is generated initially by hole transfer to the adsorbed acetone and the identity of the unstable peroxy intermediate must be $CH_3COCH_2OO^{\bullet}$.

Introduction

Photocatalytic reactions over semiconductor powders have received considerable attention in the past 10 years because of their potential applications in the degradation of a wide range of both gaseous and aqueous pollutants.[1−3] In particular, the use of titanium dioxide for the remediation of volatile organic compounds (VOCs) has several advantages as compared to traditional heterogeneous catalysts since TiO_2 operates at ambient temperature and pressures, the reaction products are usually CO_2 and water, it exhibits high corrosion resistance, and it also displays efficient photocatalytic conversion rates in contact with both liquid and gas phases. Despite the growing interests in the applications of TiO_2 for photocatalytic oxidation of gas phase organic compounds, a complete understanding of the photocatalytic mechanism is still in the early stages.

To explore the reaction mechanism of VOC decomposition in heterogeneous photocatalysis, identification of the reaction intermediates by spectroscopic methods is required under reaction conditions. Considering the role of surface orientation in the photochemical reactivity of TiO_2 (as demonstrated on both thin films[4] and polycrystalline materials[5]), it is also necessary to characterize these intermediates directly at the surface, before desorption and subsequent reactivity in the gas phase. Electron paramagnetic resonance (EPR) is a powerful spectroscopic method for exploring the site specific photochemical reactions that occur on the polycrystalline powders under in situ conditions, and the technique has been widely used in the past for the characterization of surface radical species over irradiated TiO_2.[6−14] While many paramagnetic species have been identified by this technique (O^-, O_2^-, O_3^-, $HO_2^{\bullet}$, and Ti^{3+}), the direct role and participation of some of these radicals in the photocatalytic reactions remain unclear.

In a previous study,[15] we identified several neutral surface peroxyacyl species (general formula $RCO_3^{\bullet}$), which are well-known oxidative intermediates in the initiated gas phase oxidation of aldehydes.[16] These surface radical species were generated by UV irradiation of rutile TiO_2 containing coadsorbed molecular oxygen and selected aldehydes over a dehydrated surface. In the present paper, we will provide direct evidence for the formation of a thermally unstable surface alkylperoxy radical ($ROO^{\bullet}$), formed by low temperature UV irradiation of TiO_2 containing coadsorbed acetone and O_2. The assignment of the radical intermediate to an $ROO^{\bullet}$ species has been confirmed using ^{17}O-labeled oxygen. TiO_2 surface-stabilized peroxy radicals have been identified in the past using EPR, notably with coadsorbed ethylene and O_2,[17] but this is the first identification of such an intermediate with acetone/O_2.

Experimental Section

P-25 titanium dioxide (Degussa) was used throughout this work (surface area 49 $m^2\ g^{-1}$). Prior to reaction with acetone, the polycrystalline TiO_2 powder was slowly heated (over a 5 h period) under vacuum (10^{-5} Torr) up to a maximum temperature of 823 K and held at this temperature for a further 1 h. The reduced powder (blue in color due to the excess number of Ti^{3+} centers[15]) was then exposed to oxygen (50 Torr) at 823 K and cooled to room temperature (under the oxygen atmosphere), producing a clean oxidized surface free from contaminants or surface hydroxyls. The excess oxygen was subsequently evacuated at room temperature. At no time was the sample open to the air, ensuring that the surface remains clean. While exposure of a thermally reduced TiO_2 surface to O_2 at 298 K leads to the formation of paramagnetic surface oxygen radicals (like O^-, O_2^-, or O_3^-), exposure of O_2 to the high temperature sample (823 K) leads to the formation of diamagnetic surface O^{2-} lattice anions, as the surface is effectively reoxidized at this high temperature. This was confirmed by recording the EPR spectrum of the oxidized sample, which did not display any signal.

* To whom correspondence should be addressed. Tel: 00 44(0)2920 875850. Fax: 00 44(0)2920 874030. E-mail: MurphyDM@cardiff.ac.uk.
[†] Cardiff University.
[‡] Huntsman Tioxide.

10.1021/jp022448n CCC: $25.00
Published on Web 02/20/2003

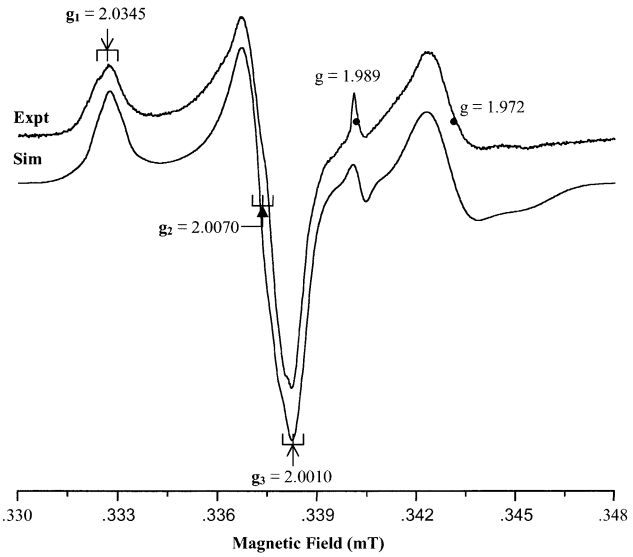

Figure 1. Experimental and simulated EPR spectrum of dehydrated P25 after UV irradiation for 30 min at 100 K in the presence of coadsorbed acetone:O_2 (10 Torr total pressure in a 10:1 ratio). The EPR spectrum was recorded at 10 K (1 T = 10^4 G).

The oxidized material was then exposed to the probe gases (10 Torr) at 298 K from a vacuum manifold. The acetone to O_2 ratio was 10:1 in these coadsorption experiments. While the acetone:O_2 ratio may be different in the adsorbed state as compared to the gaseous state, due to differences in the adsorption characteristics of the two gases on TiO_2, nevertheless, it is clear that the acetone remains in excess on the surface due to the absence of any O_2^- signal. For samples containing adsorbed oxygen only, or an oxygen rich acetone:O_2 mixture, then photoirradition of the sample would produce the characteristic O_2^- signal. After exposure of the sample to the acetone:O_2 mixture, the EPR sample cell was then placed into the EPR spectrometer at 100 K and irradiated in situ for 30 min at this temperature. The high purity O_2 gas was supplied by BOC Ltd. Acetone was of analytic grade and supplied by Aldrich Chemicals Ltd. The acetone was purified by repeated freeze−pump−thaw cycles, to remove oxygen, prior to use. ^{17}O-labeled dioxygen gas (63% enrichment) was supplied by Icon Serivces Inc. (New Jersey) and used without further purification.

A 1000 W Oriel Instruments UV lamp, incorporating a Hg/Xe arc lamp (250 nm to >2500 nm), was used for all irradiations in the presence of a water filter. The UV output below 280 nm accounts for only 4−5% of the total lamp output. The EPR spectra were recorded on a Bruker ESP 300E series spectrometer. All spectra were recorded at X-band frequencies, 100 kHz field modulation, and 5 mW microwave power. The g values were obtained using a Bruker ER035M NMR gaussmeter calibrated using the perylene radical cation in concentrated H_2SO_4 (g = 2.002 569). EPR computer simulations were performed using the SIM14S program (QCPE 265).

Results

A sample of fully dehydrated TiO_2 was UV irradiated at 100 K in the presence of coadsorbed acetone:O_2 (10:1 ratio; total pressure = 10 Torr). The sample was subsequently cooled to 10 K for EPR measurements, and the resulting spectrum is shown in Figure 1. The high field features at $g = 1.989$ and $g \approx 1.972$ can be easily assigned to Ti^{3+} cations at substitutional and normal lattice sites, respectively. The latter broad signal at $g \approx 1.972$ is actually a composite signal, with an asymmetric g tensor ($g_\perp = 1.972$ and $g_{||} = 1.960$), arising from the presence of primarily bulk Ti^{3+} centers, as widely reported in the literature.[6−9,13,15] A new low field orthorhombic signal at $g_1 = 2.0345$, $g_2 = 2.0070$, and $g_3 = 2.0010$ is also visible in the spectrum. This new signal is thermally unstable, since raising the sample temperature to 298 K followed by recooling to 10 K caused the signal to disappear. The signal could be regenerated by a subsequent UV illumination at low temperatures. This new signal was only observed in the presence of an acetone rich mixture with coadsorbed oxygen. Irradiation of the sample containing acetone only did not produce the new spectrum. In addition, irradiation of the sample under oxygen only (or under an oxygen rich CH_3COCH_3:O_2 mixture) produced the well-known spectrum of the superoxide O_2^- radical (spectrum not shown) stable to temperatures in excess of 400 K. In other words, the new radical species formed from adsorbed acetone/O_2 contains oxygen but does not arise from the O_2^- radical. It should be clearly stated that this new radical could also be generated on a hydrated TiO_2 surface, although better spectral resolution and intensity was obtained on the dehydrated material.

Closer inspection of the signal in Figure 1 reveals the presence of a small hyperfine structure superimposed on each of the three g values. This hyperfine structure was more easily observed by recording the second derivative EPR signal and by computer simulation of the EPR spectrum (shown in Figure 1). The presence of the hyperfine structure was also confirmed using deuterated acetone (CD_3COCD_3), where a pronounced narrowing of the line width was observed (the ratio of the magnetic moments of deuterium to hydrogen is $\mu_D/\mu_H = 0.15$ so a smaller triplet pattern from deuterium is expected, which is often unresolved). The EPR spectrum was best simulated using two equivalent $I = 1/2$ nuclei ($^HA_1 = 0.34$ mT, $^HA_2 = 0.10$ mT, $^HA_3 = 0.29$ mT, and $a_{iso} = 0.243$ mT), since the addition of three equivalent $I = 1/2$ nuclei produced an unsatisfactory fit. This indicates the presence of a $-CH_2-$ fragment weakly interacting with the unpaired electron spin.

To obtain further information on the nature and identity of the new radical species in Figure 1, experiments were carried out using labeled ^{17}O. The activated TiO_2 sample was subsequently irradiated at low temperature using coadsorbed CH_3COCH_3:$^{17}O_2$, and the resulting spectrum is shown in Figure 2. The relative abundance of the isotopmers ($^{16}O_2$, $^{17}O^{16}O$, and $^{17}O_2$) present in the gas mixture can be easily calculated;[18] therefore, with a 63% enrichment level, the six line hyperfine pattern from the $I = 5/2$ nucleus of $^{17}O^{16}O$ is expected to dominate the EPR spectrum, with much smaller contributions from $^{16}O_2$ and $^{17}O_2$. As a result, the intensity of the EPR spectrum is now distributed primarily over six lines so that the spectrum appears less intense as compared to the Ti^{3+} signal. For comparison purposes, the EPR spectrum of ^{17}O-labeled O_2^- was also generated on the same activated TiO_2 surface (spectrum not shown) producing the well-known and widely reported six and 11 line hyperfine patterns of $(^{17}O^{16}O)^-$ and $(^{17}O^{17}O)^-$ respectively, with the largest splitting of $A_{xx} = 7.6$ mT. The hyperfine pattern observed in Figure 2 is clearly not that expected of $^{17}O_2^-$. Closer analysis of the spectrum reveals the presence of two sextets with $^{17O}A_{||}$(i) = 9.45 mT and $^{17O}A_{||}$(ii) = 5.52 mT both centered on the g_3 (or g_{xx}) component at 2.0010; see Table 1.

Discussion

A number of paramagnetic oxygen-centered radicals can be formed on the TiO_2 surface, including O^-, O_2^-, O_3^-, $OH^\bullet$, and

TABLE 1: Spin Hamiltonian Parameters for a Selection of Oxygen-Centered Radicals Formed on the TiO_2 Surface

species	g_1	g_2	g_3	$^{17O}A_{\|\|}$(i)[a]	$^{17O}A_{\|\|}$(ii)[a]	comment	ref
O^-	2.026	2.026	2.002				6
O_2^-	2.025	2.008	2.0016				6
O_3^-	2.017	2.011	2.001				19
$HO_2^\bullet$	2.034	2.008	2.002			hydrated surface	26
$RCO_3^\bullet$	2.017	2.008	2.003			coadsorbed aldehyde/O_2	15
$ROO^\bullet$	2.034	2.010	2.001	9.5	3.5	coadsorbed ethylene/O_2	17
$ROO^\bullet$	2.0345	2.0070	2.0010	9.45	5.52	coadsorbed acetone/O_2	this work

[a] ^{17}O hyperfine couplings in mT.

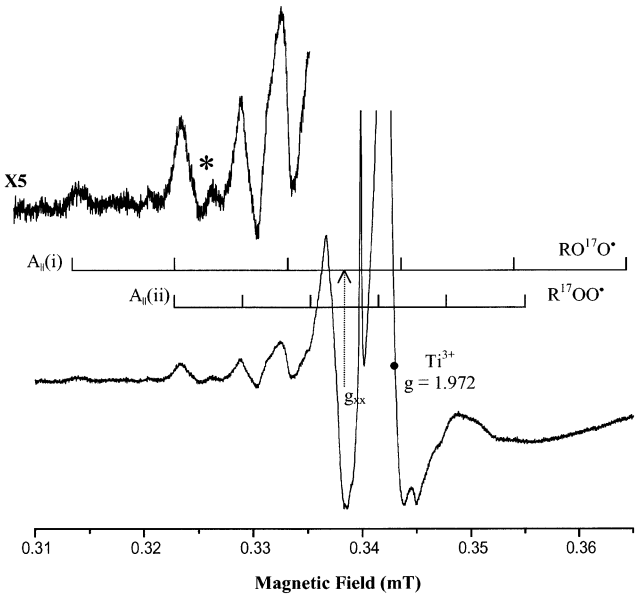

Figure 2. Experimental EPR spectrum of dehydrated P25 after UV irradiation for 30 min at 100 K in the presence of coadsorbed acetone and ^{17}O-labeled oxygen of 63% isotopic enrichment (10 Torr total pressure in a 10:1 ratio). The EPR spectrum was recorded at 10 K. The peak marked * is due to one transition from traces of $^{17}O_2^-$.

$HO_2^\bullet$ and $ROO^\bullet$ radicals. The g values for the O^-, O_2^-, and O_3^- radicals are well-known (Table 1) and can be immediately eliminated as possible candidates for the new radical species in Figures 1 and 2, since they have no intrinsic hyperfine interaction with a proton. It is possible for a superhyperfine interaction to produce a small coupling in the spectrum (e.g., $OH_{surf}\cdots O_2^-$) but, as stated above, the observed ^{17}O hyperfine pattern (Figure 2) is not typical of $^{17}O^-$, $^{17}O_2^-$, or $^{17}O_3^-$.[19] For comparison, we have also generated the $HO_2^\bullet$ radical on a fully hydrated TiO_2 surface (spectrum not shown) and the large characteristic coupling from the single proton can be clearly seen. While $HO_2^\bullet$ is also thermally unstable, the g values are distinctly different from the new radical intermediate (Table 1) and so cannot account for the signal in Figures 1 and 2. The $OH^\bullet$ radical is an extremely reactive, short-lived intermediate and cannot be directly observed by EPR on the TiO_2 surface, even at 10 K. It can be indirectly identified through spin trapping experiments or through analysis of the secondary radicals formed by the reactions of $OH^\bullet$.[20] Nevertheless, the spin Hamiltonian parameters of $OH^\bullet$ are very well-known[21] and are very different to those of the acetone intermediate observed in this work.

The next likely candidate to explain the origin of the new signal is a surface peroxy radical ($ROO^\bullet$). Sevilla et al.[22] have conducted an extensive study of carbon-based peroxyl radicals and reported that the g values vary only slightly from $g_1 = 2.035$, $g_2 = 2.008$, and $g_3 = 2.003$; the greatest deviation was found for the crystal field sensitive g_1 component. The stability of these radicals is known to be highly sensitive to the terminal oxygen spin density, and according to McCain and Palke,[23] the average g values of $ROO^\bullet$ radicals depend on the electronic structure of the R group. In this case, the average g value for the new radical is 2.014, which is in the range typical of alkylperoxy radicals. The spin density in the peroxy radical is localized primarily in the p_z orbital of the two oxygens. The hyperfine coupling on the terminal oxygen ($RO^{17}O^\bullet$) is usually labeled $A_{||}$(i), while coupling from the inner oxygen ($R^{17}OO^\bullet$) is labeled $A_{||}$(ii). From analysis of the spectrum in Figure 2, the hyperfine couplings were determined as $A_{||}$(i) = 9.45 mT and $A_{||}$(ii) = 5.52 mT. Anisotropic hyperfine couplings from spin densities in such p_z orbitals should follow approximate axial symmetry with $A_{||} = (a + 2B)\rho^\pi$ and $A_\perp = (a - B)\rho^\pi$, where ρ is the spin density in the p_z orbital. Because of the strong overlapping signal from Ti^{3+}, an accurate value for $A_\perp$ could not be obtained but is expected to be very small. A good estimate of the spin density distribution in the p_z orbitals can then be obtained from the relation $\rho^\pi(i) = |A_{||}(i)|/15.4$ mT, 15.4 mT $= |a + 2B|$ using the $A_{||}$ value only.[22] From this relation, we estimate that the terminal oxygen spin density value is 0.61 as expected for a peroxy radical. Indeed, stable surface methylperoxy and propylperoxy species have been observed by EPR at 100 K on MgO[24] and Bi_2O_3,[25] respectively, and terminal oxygen spin densities have been measured in the range $\rho_\pi = 0.70-0.61$.

Because the sum of the two $A_{||}$ couplings (i and ii) for carbon-based peroxy radicals is nearly constant, this suggests that little spin density is delocalized into the R group of $ROO^\bullet$.[22] However, computer simulations of the EPR spectrum in Figure 1 revealed the presence of a small almost isotropic hyperfine coupling (a_{iso} = 0.243 mT) with two equivalent protons (i.e., two $I = 1/2$ nuclei). This coupling is far smaller than the observed proton couplings in $HO^\bullet$ ($A_1 = A_3 = 0$ mT, $A_2 = 5.7$ mT, $a_{iso} = 1.9$ mT[21]) and $HO_2^\bullet$ ($A_1 = 1.2$ mT, $A_2 = 1.2$ mT, $A_3 = 1.4$ mT, $a_{iso} = 1.2$ mT[26]) where the proton is directly attached to the oxygen atoms, rather than through a C−O bond. The observation of this hyperfine pattern in Figure 1 suggests that R is an alkyl species (also confirmed by the average g value of 2.014[17]) and eliminates the possibility of a $-CH-$ or $-CH_3$ fragment attached to $-OO^\bullet$. In other words, the evidence strongly supports the assignment of the new radical to an alkylperoxy species of the form $R-CH_2OO^\bullet$.

On the basis of the above findings, the mechanism of radical formation can now be considered. In the case of adsorbed acetone, electron transfer from the surface to the adsorbed organic molecule can occur resulting in population of the lowest unoccupied π_{CO}* molecular orbital forming an acetone ketyl radical[27]

$$(CH_3)_2CO + e^- \rightarrow (CH_3)_2CO^{\bullet -} \qquad (1)$$

This is unlikely to occur as the ketyl radical is expected to be a more powerful reductant than a surface-trapped electron ($(CH_3)_2CO/(CH_3)_2C^\bullet OH = -1.81$V vs NHE).[28] Furthermore,

while the resulting acyl ($CH_3CO^{\bullet}$) and methyl radicals ($^{\bullet}CH_3$) resulting from ketyl fragmentation could conceivably react with oxygen to form peroxy radicals ($CH_3CO-OO^{\bullet}$ and $CH_3-OO^{\bullet}$), the spectroscopic features observed in Figures 1 and 2 are not consistent with such as assignment.

It is also possible that electron transfer occurs to surface-trapped holes, O^- centers (created during the course of UV irradiation), or Ti^{3+}, producing an adsorbed cation radical. This will quickly deprotonate by H^+ transfer to the surface oxide, producing the propanone radical. Both steps are summarized according to eq 2.

$$CH_3COCH_3 + O^- \rightarrow CH_3COCH_2^{\bullet} + OH^- \qquad (2)$$

A similar reaction will occur between acetone and the hydroxyl radicals.[29] The propanone radical can then react with oxygen forming the peroxy radical according to eq 3.

$$CH_3COCH_2^{\bullet} + O_2 \rightarrow CH_3COCH_2OO^{\bullet} \qquad (3)$$

Because the rate of hole transfer is believed to be much faster than the rate of electron transfer across the interface (e.g., 100 ns vs several milliseconds, respectively), $CH_3COCH_2^{\bullet}$ radicals may be formed on the surface. Molecular oxygen addition to these radicals would also produce a peroxy radical ($CH_3COCH_2-OO^{\bullet}$) and because the CO group is not directly attached to the O−O group, g_1 values typical of alkyl-centered peroxy radicals ($g_1 = 2.035$) may still be seen. Furthermore, it should be recalled that the EPR spectrum obtained using $^{16}O_2$ indicated the presence of only two weakly interacting protons, as expected for an $R-CH_2-OO^{\bullet}$ fragment. Therefore, the mechanistic considerations support the spectroscopic evidence on the identity of the radical intermediate as $CH_3CO-CH_2OO^{\bullet}$.

Conclusion

To conclude, EPR spectroscopy was used to study the nature of the radical intermediate formed in the initial stages of acetone oxidation over UV-irradiated TiO_2. The intermediate was only formed and stabilized at temperatures below 150 K. Using ^{17}O-labeled dioxygen, the radical intermediate was identified as a peroxy-based radical ($ROO^{\bullet}$), while the well-resolved EPR spectrum obtained with $^{16}O_2$ indicated the presence of a $-CH_2-$ fragment in the R group. On the basis of this evidence, the alklyperoxy radical was confirmed as $CH_3COCH_2OO^{\bullet}$, generated by hole transfer to adsorbed acetone. Under the adopted conditions of coadsorbed acetone:O_2, no ionic molecular oxygen radicals (such as O_2^- or O_3^-) are formed.

Acknowledgment. Funding of the national ENDOR facility by EPSRC (Grant No. GR/R17980/01) is gratefully acknowledged. A.L.A. thanks Huntsman Tioxide for support as a CASE award.

References and Notes

(1) Fox, M. A.; Dulay, M. T. *Chem. Rev.* **1993**, *93*, 341.

(2) Linsebigler, A. L.; Lu, G. Q.; Yates, J. T. *Chem. Rev.* **1995**, *95*, 735.

(3) Hofmann, M. R.; Martin, S. T.; Choi, W.; Bahnemann, D. W. *Chem. Rev.* **1995**, *95*, 69.

(4) Morris Hotsenpiller, P. A.; Bolt, J. D.; Farneth, W. E.; Lowekamp, J. B.; Roher, G. S. *J. Phys. Chem. B* **1998**, *102*, 3216.

(5) Lowekamp, J. B.; Roher, G. S.; Morris Hotsenpiller, P. A.; Bolt, J. D.; Farneth, W. E. *J. Phys. Chem. B* **1998**, *102*, 7323.

(6) Howe, R. F.; Gratzel, M. *J. Phys. Chem.* **1985**, *89*, 4495.

(7) Howe, R. F.; Gratzel, M. *J. Phys. Chem.* **1987**, *91*, 3906.

(8) Anpo, M.; Shima, T.; Kubokawa, Y. *Chem. Lett.* **1985**, 1799.

(9) Micic, O. I.; Zhang, Y.; Cromack, K. R.; Trifunac, A. D.; Thurnauer, M. C. *J. Phys. Chem.* **1993**, *97*, 7277.

(10) Micic, O. I.; Zhang, Y.; Cromack, K. R.; Trifunac, A. D.; Thurnauer, M. C. *J. Phys. Chem.* **1993**, *97*, 13284.

(11) Rajh, T.; Ostafin, A. E.; Micic, O. I.; Tiede, D. M.; Thurnauer, M. C. *J. Phys. Chem.* **1996**, *100*, 4538.

(12) Nosaka, Y.; Koenuma, K.; Ushida, K.; Kira, A. *Langmuir* **1996**, *12*, 736.

(13) Coronado, J. M.; Maira, A. J.; Conesa, J. C.; Yeung, K. L.; Augugliaro, V.; Soria, J. *Langmuir* **2001**, *17*, 5368.

(14) Maira, A. J.; Yeung, K. L.; Soria, J.; Coronado, J. M.; Belver, C.; Lee, C. Y.; Augugliaro, V. *Appl. Catal. B* **2001**, *29*, 327.

(15) Jenkins, C. A.; Murphy, D. M. *J. Phys. Chem. B* **1999**, *103*, 1019.

(16) Clinton, N. A.; Kenley, R. A.; Traylor, T. G. *J. Am. Chem. Soc.* **1975**, *97*, 3746.

(17) Gonzalez-Elipe, A. R.; Che, M. *J. Chim. Phys.* **1982**, *79*, 355.

(18) Chiesa, M.; Giamello, E.; Paganini, M. C.; Sojka, Z.; Murphy, D. M. *J. Chem. Phys.* **2002**, *116*, 4266.

(19) (a) Che, M.; Tench, A. J. *Adv. Catal.* **1982**, *31*, 77. (b) Che, M.; Tench, A. J. *Adv. Catal.* **1983**, *32*, 1.

(20) Jenkins, C.; Murphy, D. M.; Rowlands, C. C.; Egerton, T. A. *J. Chem. Soc., Perkin Trans 2* **1997**, 2479.

(21) Giamello, E.; Calosso, L.; Fubini, B.; Geobaldo, F. *J. Phys. Chem.* **1993**, *97*, 5735.

(22) Sevilla, M. D.; Becker, D.; Yao, M. *J. Chem. Soc., Faraday Trans.* **1990**, *86*, 3279.

(23) McCain, D. C.; Palke, W. E. *J. Magn. Reson.* **1975**, *20*, 52.

(24) Ito, T.; Wang, Y. X.; Lin, C. H.; Lunsford, J. H. *J. Am. Chem. Soc.* **1985**, *107*, 5062.

(25) Driscoll, D. J.; Campbell, K. D.; Lunsford, J. H. *Adv. Catal.* **1987**, *35*, 139.

(26) Catton, R. C.; Symons, M. C. R. *Inorg. Phys. Theor.* **1969**, 1393.

(27) Lai, C. C.; Freeman G. R. *J. Phys. Chem.* **1990**, *94*, 302.

(28) Wardman, P. *J. Phys. Chem. Ref. Data* **1989**, *18*, 1637.

(29) DeMore, W. B.; Sander, S. P.; Golden, D. M.; Hampson, R. F.; Kurylo, M. J.; Howard, C. J.; Ravishankara, A. R.; Kolb, C. E.; Molina, M. J. *JPL Publ.* **1997**, *97*, 1.